


Grhl3 modulates epithelial structure formation of the circumvallate papilla during mouse development

Nirpesh Adhikari¹ · Sanjiv Neupane¹ · Gi-Jeong Gwon¹ · Ji-Youn Kim² · Chang-Hyeon An³ · Sanggyu Lee⁴ · Wern-Joo Sohn¹ · Youngkyun Lee¹ · Jae-Young Kim¹ 

Accepted: 26 August 2016 / Published online: 1 September 2016
© Springer-Verlag Berlin Heidelberg 2016

Abstract Grainyhead-like 3 (*Grhl3*) is a transcription factor involved in epithelial morphogenesis. In the present study, we evaluated the developmental role of *Grhl3* in structural formation of the circumvallate papilla (CVP), which undergoes dynamic morphological changes during organogenesis. The specific expression pattern of *Grhl3* was examined in the CVP-forming region, specifically in the apex and epithelial stalk from E13.5 to E15.5 using in situ hybridization. To determine the role of *Grhl3* in epithelial morphogenesis of the CVP, we employed an in vitro tongue culture method, wherein E13.5 tongue were isolated and cultured for 2 days after knocking down of *Grhl3*. Knockdown of *Grhl3* resulted in significant changes to the epithelial structure of the CVP, such that the apical region of the CVP was smaller in size, and the epithelial stalks were more deeply invaginated. To define the mechanisms

underlying these morphological alterations, we examined cell migration, proliferation, and apoptosis using phalloidin staining, immunohistochemistry against Ki67, ROCK1, and E-cadherin, and a TUNEL assay, respectively. These results revealed an increase in proliferation, a reduction in apoptosis, and an altered pattern of cytoskeletal formation in the CVP-forming epithelium, following *Grhl3* knockdown. In addition, there were changes in the specific expression patterns of signaling and apoptosis-related molecules such as *Axin2*, *Bak1*, *Bcl2*, *Casp3*, *Casp8*, *Ctnnb1*, *Cnnd1*, *Gli3*, *Lef1*, *Ptch1*, *Rock1*, *Shh*, and *Wnt11*, which could explain the altered cellular and morphological events. Based on these results, we propose that developmental stage-specific *Grhl3* plays a significant role in CVP morphogenesis not by just disruption of epithelial integrity but by regulating epithelial cell proliferation, apoptosis, and migration via *Shh*, *Wnt*, and apoptosis signaling during mouse embryogenesis.

Nirpesh Adhikari and Sanjiv Neupane have contributed equally to this work.

Electronic supplementary material The online version of this article (doi:10.1007/s00418-016-1487-7) contains supplementary material, which is available to authorized users.

✉ Jae-Young Kim
jykim91@knu.ac.kr

¹ Department of Biochemistry, School of Dentistry, IHBR, Kyungpook National University, 2177, Dalgubeol-daero, Jung-gu, Daegu 41940, Korea

² Department of Dental Hygiene, Gachon University College of Health Science, Incheon, Korea

³ Department of Oral and Maxillofacial Radiology, School of Dentistry, IHBR, Kyungpook National University, Daegu, Korea

⁴ School of Life Science and Biotechnology, Kyungpook National University, Daegu, Korea

Keywords Epithelial morphogenesis · Rearrangement · Cytoskeletal formation · Morphogenesis · Grainyhead-like 3

Introduction

Epithelial appendages such as the feather, hair, tooth, whiskers, and mammary gland share similar morphogenetic events during the early stages of their development (Mikkola 2007). They all undergo induction, epithelial thickening (placode formation), and bud formation, resulting in either protrusion from or invagination into an epithelial surface that later converts into different adult structures (Biggs and Mikkola 2014). Circumvallate papilla (CVP) formation is an excellent model system for studying epithelial morphogenesis. The CVP initially develops from

a thickening of the dorsal epithelium that forms a central “dome-shaped” structure with a mesenchymal core. Adjacent to the central dome are two epithelial stalks that invaginate into the underlying mesenchyme and give rise to the von Ebners’ minor salivary gland (VEG) (Jitpuk-deebodintrat et al. 2002). The formation of these structures involves a series of sequential and reciprocal interactions between the epithelium and the underlying mesenchyme, which are mediated by a number of conserved signaling pathways including the Wnt, fibroblast growth factor (Fgf), transforming growth factor β (Tgf β), and hedgehog (Hh) families, along with their downstream transcription factors (Pispa and Thesleff 2003).

Among these different signaling pathways, Sonic hedgehog (*Shh*) was shown to be involved in the induction and morphogenesis of early CVP and salivary gland development (Jaskoll et al. 2004; Lee et al. 2006). In addition, the interaction of *Shh* with another important molecule, *Wnt11* (from the Wnt signaling pathway), is responsible for dome and lateral trench wall formation during CVP development (Kim et al. 2009). The involvement of several other signaling molecules and transcription factors, including *Fgf10*, *Pax9*, *Six1*, *Six4*, *Eda*, and *WT1*, has been examined (Petersen et al. 2011; Suzuki et al. 2011; Wells et al. 2011; Kist et al. 2014; Gao et al. 2014); however, the integrated regulatory mechanisms that underlie epithelial structure formation in the CVP remain to be elucidated. To begin unraveling the complex molecular interactions involved in CVP formation, we evaluated the developmental function of Grainyhead-like 3 (*Grhl3*), which is known to play an important role in epithelial organogenesis.

Grhl3, one of the three mammalian homologs of the *Drosophila* transcription factor grainyhead, has been reported to be essential for epidermal development, migration, and integrity (Ting et al. 2005a, b; Hislop et al. 2008; Boglev et al. 2011). In addition, it is known to regulate cell apoptosis, oral periderm development, and neural tube closure (Gustavsson et al. 2008; Lukosz et al. 2011; De la Garza et al. 2013; Peyrard-Janvid et al. 2014; Liu et al. 2016). Furthermore, while *Grhl3* is known to be a key regulator of epithelial cell rearrangement, its specific role in structure formation during organogenesis has yet to be elucidated.

In the current study, we examined the precise expression pattern and developmental roles of *Grhl3* during CVP development. We showed that developmental stage-specific *Grhl3* is involved in epithelial cell proliferation, apoptosis, and migration to achieve the proper structural formation of CVP. Precise coordination of these events controls the cellular rearrangements and dramatic morphological changes that result in typical structure formation of the CVP.

Materials and methods

All experiments were performed according to the guidelines of the Kyungpook National University, School of Dentistry, Intramural Animal Use and Care Committee.

Animals

Adult ICR mice were housed in a temperature-controlled room (22 °C) under artificial illumination (lights on from 05:00 to 17:00), at 55 % relative humidity, with free access to food and water. Mouse embryos were obtained from time-mated pregnant mice. The day on which a vaginal plug was confirmed was designated as embryonic day 0 (E0).

In situ hybridizations

Whole-mount and section in situ hybridizations were performed at 68 °C using digoxigenin (DIG)-labeled RNA probes following standard protocols, as described previously (Neupane et al. 2015). Following whole-mount in situ hybridization, 20- μ m thick frontal frozen sections were prepared to examine the detailed expression pattern of *Grhl3*.

In vitro organ cultivations

Tongues of embryonic mice were micro-dissected from the mandible at E13.5 under a dissecting microscope in cold phosphate-buffered saline (PBS) and were cultured for 2 days using Trowell’s modified culture method, as previously described (Neupane et al. 2015). To examine changes in gene expression, dissected tongues were cultivated using a roller culture method as previously described (Sohn et al. 2015). During in vitro organ culture, antisense oligodeoxynucleotides (AS-ODNs) for *Grhl3* were added to the medium at a final concentration of 1 μ M as previously described (Sohn et al. 2012). The sequences of ODNs were as follows: antisense AS-ODN 5'- CTCCTCTGTCTCC-CTCCTCA-3' and sense (S)-ODN 5'-TGAGGAGGGA-GACAGAGGAG-3'. In addition, scrambled ODN was examined as a control of experiment (data not shown). To confirm the AS-ODN experiment, we also employed the siRNA system, purchased from Ambion (ID: 106644).

Slice cultivation and DiI labeling

Slice cultivation and DiI labeling were performed as previously described (Neupane et al. 2015). After microdissection of the E14 tongue, 100- μ m frontal sections of the CVP were prepared using a

vibratome (VT1000S, Leica, Germany). The fluorescent carbocyanine dye DiI (1,1'-dioctadecyl-3,3',3',3'-tetramethylindocarbocyanine perchlorate; Cat. no. C-7001; Life Technologies, USA) was microinjected to the trench region of the exposed CVP in the slice section of tongue. Tissues were incubated over an agarose gel containing DMEM for 48 h.

Histology and immunohistochemistry

Histology and immunostaining were carried out as previously described (Neupane et al. 2015). Primary antibodies used were Ki67 (Cat. no. RM-9106, Thermo Scientific, Fremont, CA, USA), ROCK1 (Cat. no. ab45171, Abcam, UK), and E-cadherin (Cat. no. AF748; R&D Systems, USA). At least 12 slides from over 30 specimens for each control and experimental group were randomly selected for immunostaining against Ki67, and the number of positive cells were counted in the epithelium designating as apex, trench, and vallum, respectively.

Three-dimensional reconstructions

Three-dimensional reconstructions were performed as previously described (Sohn et al. 2011). Reconstruction software, which can be downloaded from <http://synapses.clm.utexas.edu/tools/reconstruct/reconstruct.stm> (August 20, 2007), was used to produce 3D images of the CVP.

Phalloidin staining

Phalloidin staining was performed as previously described (Neupane et al. 2015). Briefly, frozen sections were washed with PBS, permeabilized with 0.1 % Triton X-100 in PBS, and incubated with phalloidin-fluorescein isothiocyanate (Cat no. p5282; Sigma Aldrich, USA) at room temperature for 1 h, then visualized using a fluorescence microscope (DM-2500; Leica, Germany).

TUNEL assay

A terminal deoxynucleotidyl transferase-mediated dUTP nick-end labeling (TUNEL) assay was performed as previously described (Sohn et al. 2012) using an in situ cell apoptosis detection kit (Cat. no. 4810-30-K, Trevigen, MD., USA) according to the manufacturer's instructions. DAB substrate was used to detect sites of in situ apoptosis under a light microscope. At least 12 slides from over 30 specimens for each control and experimental group were randomly selected for TUNEL assay, and the number of positive cells were counted in the epithelium designating as apex, trench, and vallum.

Real-time quantitative polymerase chain reaction

RT-qPCR was performed as previously described (Neupane et al. 2015). After 24 h cultivation at E13.5, CVP-forming tissue was dissected and harvested the RNA to synthesis cDNA. Results for each sample were normalized to Hprt and expressed as a fold change. Table 1 lists the primer sequences used in this study. Data were expressed as mean \pm SD. Mean expression levels were compared between the experimental and control groups using Student's *t* test. *P* values <0.05 were considered significant.

Results

Expression pattern of *Grhl3* in the developing circumvallate papilla

In order to determine the precise expression pattern of *Grhl3*, in situ hybridization was performed at E13.5, E14.5, and E15.5, since these stages show remarkable changes in the structure of the CVP (Fig. 1). At E13.5, when the CVP is beginning to evaginate from the epithelial surface, *Grhl3* expression was observed in the thickened epithelium (Fig. 1a, b). This was confirmed in a frontal section showing expression in the superficial layer of the thickened epithelium of the CVP (Fig. 1c). At E14.5, the CVP is a much more prominent protuberance of the epithelium, and *Grhl3* expression was strong at this stage (Fig. 1d, e). In addition, *Grhl3* expression was observed in the developing funghi-form papillae along the median sulcus at E14.5 (Fig. 1d). The CVP comprises a raised dome structure enclosing condensed mesenchyme with an invaginated epithelial stalk forming the trench. Section in situ hybridisation revealed strong *Grhl3* expression in the CVP apex and trench epithelium, but no expression in the mesenchymal core (Fig. 1f). At E15.5, the CVP dome is much larger compared to that at E14.5, and *Grhl3* expression was still strong (Fig. 1g, h). Section in situ hybridization at E15.5 revealed a much larger CVP dome and more deeply invaginated epithelial stalks, with *Grhl3* expression still restricted to the apex and trench epithelium of the CVP (Fig. 1i). The same expression pattern was observed in the CVP at E14.5 and E15.5 which was confirmed in the frontal sections of the whole-mount in situ hybridization (data not shown).

Functional analysis after *Grhl3* knockdown during in vitro organ cultivation

In order to evaluate the role of *Grhl3* in CVP morphogenesis, we cultured tongue with AS-ODNs to knockdown *Grhl3*. We used E13.5 tongue, a stage when *Grhl3* is expressed; however, major morphological changes in the

Table 1 Primer sequences for RT-qPCR

Gene	Accession	Primer sequence	References	Product size (bp)	Remarks	
<i>Axin2</i>	BC057338.1	Forward	TGAAGAAGAGGAGTGGACGT		115	Wnt signaling
		Reverse	AGCTGTTTCCGTGGATCTCA			
<i>Bak1</i>	NM_007523.2	Forward	AACAGCATCTTGGGTCAGGT	Sohn et al. (2012)	82	Apoptosis signaling
		Reverse	TCTGGAACTCTGTGTCGTAG			
<i>Bcl2</i>	NM_009741.5	Forward	TGACTTCGCAGAGATGTCCA	Sohn et al. (2012)	91	Apoptosis signaling
		Reverse	ATCCCTGAAGAGTTCCTCCA			
<i>Casp3</i>	NM_001284409.1	Forward	AGACAGACAGTGGGACTGAT	Sohn et al. (2012)	93	Apoptosis signaling
		Reverse	AGTAACCAGGTGCTGTAGAG			
<i>Casp8</i>	NM_009812.2	Forward	ATCCACACAAGAAGCAGGA	Sohn et al. (2012)	93	Apoptosis signaling
		Reverse	AGACAGATTGCCTTCCTCCA			
<i>Cnd1</i>	NM_007631.2	Forward	TGCGTGCAGAAGGAGATTGT	Neupane et al. (2015)	95	Wnt signaling
		Reverse	AAGACCTCCTCTTCGCACTT			
<i>Ctnnb1</i>	NM_007614.3	Forward	TGACCTGATGGAGTTGGACA	Neupane et al. (2015)	104	Wnt signaling
		Reverse	TGGCACCAGAATGGATTCCA			
<i>Gli3</i>	NM_008130.2	Forward	CATCCACCCTGCTCCAACAT		99	Shh signaling
		Reverse	GAGGACTCAGAAGGGCCAGA			
<i>Grhl3</i>	NM_001013756.1	Forward	GCAAGCGAGGCATCCTGGTTAA		61	
		Reverse	ACGTGGTTGCTGTAGTGTGG			
<i>Lef1</i>	NM_010703.4	Forward	ACAGCGACGAGCACTTTTCT	Neupane et al. (2015)	82	Shh signaling
		Reverse	TGTCTGGACATGCCTTGCTT			
<i>Ptch1</i>	NM_008957.2	Forward	CGGACCGGGACTATCTGCAC		75	Shh signaling
		Reverse	CCTTCCCCTTGAAATCTGCT			
<i>Rock1</i>	NM_009071.2	Forward	GGTATCGTCACAAGTAGCAG-CATCA	Otsu et al. (2011)	140	Wnt signaling
		Reverse	TAAACCAGGGCATCCAATCCA			
<i>Shh</i>	NM_009170.3	Forward	CAGCGCGTGTACGTGGTGGC	Neupane et al. (2015)	335	Shh signaling
		Reverse	GGAGCGTCGGCAGCACCTG			
<i>Wnt11</i>	NM_001285792.1	Forward	CAACCTCGCAGGCGGC		150	Wnt signaling
		Reverse	AAAGAG CAGAG C CTC G CAG			
<i>Hprt</i>	NM_013556.1	Forward	CCTAAGATGATCGCAAGTTG	Neupane et al. (2014)	86	Internal standard
		Reverse	CCACAGGGACTAGAACACCT-GCTAA			

CVP have not yet occurred. After 1 day in vitro culture with AS-ODN treatment, *Grhl3* expression in the CVP was reduced by approximately 50 % (Fig. 2i) compared to the control, as measured using RT-qPCR. In addition, the section in situ hybridization after 2 days of in vitro culture also confirmed the knocking down of *Grhl3* expression (Supplementary Fig. 1). Hematoxylin and eosin staining of frontal sections through the cultured CVP showed a more rounded apex (asterisk in Fig. 2a, e) and a more invaginated trench epithelium (arrows in Fig. 2a, e) in the AS-ODN-treated specimens (Fig. 2e), compared to controls (Fig. 2a). In addition, computer-aided three-dimensional (3D) reconstructions of the CVP showed a remarkable alteration in morphology. The oral view of the 3D images of AS-ODN-treated specimens showed smaller size of the CVP dome (Fig. 2f), compared to control specimens

(Fig. 2b). The antero-posterior width of the CVP dome was reduced in the AS-ODN-treated specimens (Fig. 2g) compared to controls (Fig. 2c). Furthermore, the aboral view of 3D images of the AS-ODN-treated specimens showed deeper mesenchymal core as a result of more invaginated trench epithelium (Fig. 2h) when compared to control specimens which showed shallow mesenchymal core (Fig. 2d).

In vitro slice cultivation and cellular rearrangement

Cellular rearrangement is an important part of morphogenesis, especially during epithelial structure formation. The CVP exhibits a typical epithelial morphology; therefore, we wanted to explore the cell dynamics that lead to formation of this invaginated epithelial structure. We used

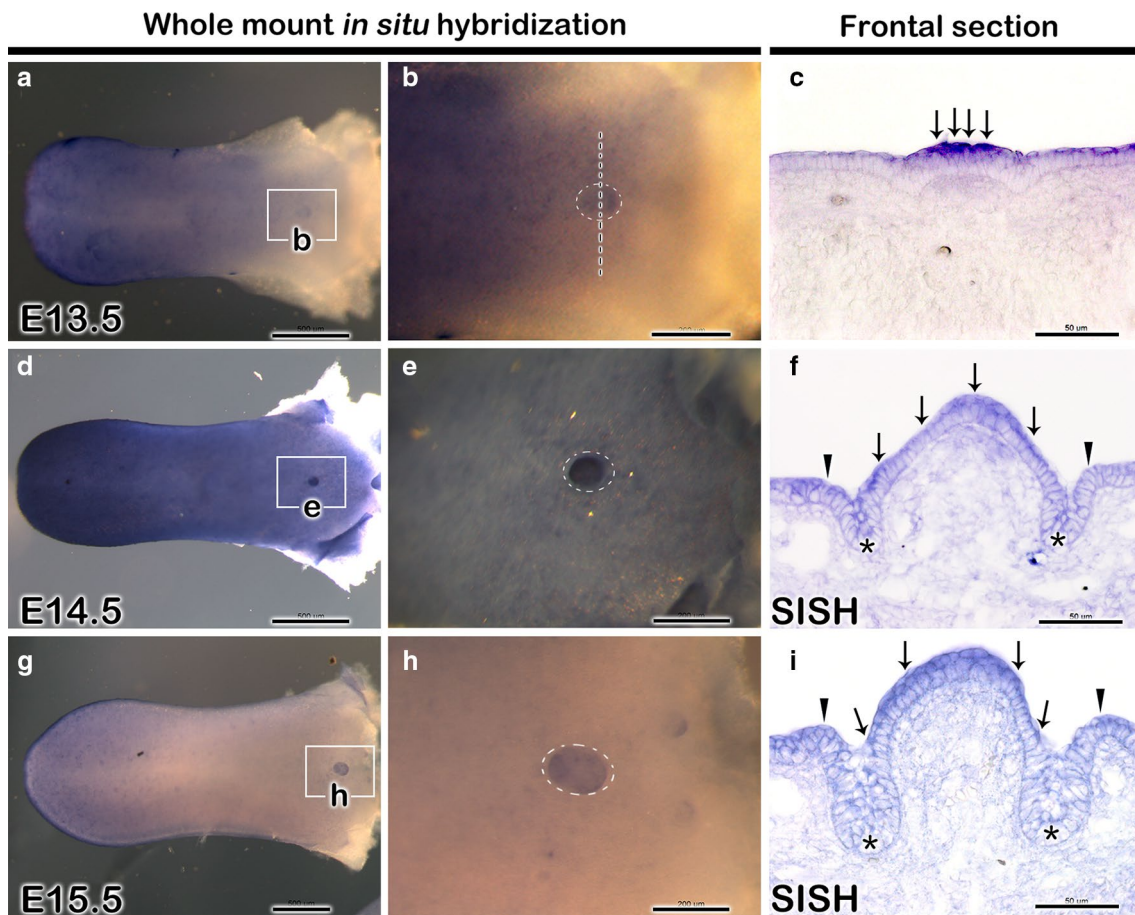


Fig. 1 *Grhl3* expression in the developing CVP. Whole-mount and section in situ hybridization using a DIG-labeled *Grhl3* mRNA probe: At E13.5, *Grhl3* is expressed in the epithelium of the CVP region (a, b), as detected by whole-mount in situ hybridization. A frozen frontal section shows expression in the upper layer of the thickened epithelium (c). At E14.5 and E15.5, whole-mount in situ hybridization shows stronger expression of *Grhl3* in the CVP (d, e, g, h). Section in situ hybridization at E14.5 and E15.5 shows expression

in the apex and trench epithelium of the CVP (f, i). White boxes represent the magnified region (b, e, h), dotted circles (b, e, h) outline the CVP and dotted line (b) indicates the level of the section. SISH, section in situ hybridization. Arrows indicate expression, arrowheads and asterisks represent the vallum and trench epithelium, respectively. Scale bars 500 µm (a, d, g), 200 µm (b, e, h), and 50 µm (c, f, i)

the lipophilic dye DiI to track cells during invagination of the trench epithelium. Cells in the trench epithelium of exposed CVP slice were labeled with DiI at E14, when the invagination was just commencing, and the tissue was transferred to in vitro slice culture. After 48 h, the patch of DiI-labeled cells in the AS-ODN-treated tissues (Fig. 3d–f) had extended upward to the trench walls and downwards to the base of the trench, resulting in an increased epithelial thickness compared to controls (Fig. 3a–c).

Altered cellular events after AS-ODN treatment against *Grhl3*

To evaluate the effects of *Grhl3* knockdown on cell proliferation and apoptosis, we used immunostaining for Ki67 and a TUNEL assay, respectively. E13.5 CVPs were

cultured in the presence or absence of AS-ODNs against *Grhl3*. After 2 days the number of Ki67 positive cells was increased in the CVP apex, trench wall, and vallum epithelium in AS-ODN-treated tissues (Fig. 4c) compared to controls (Fig. 4a). The number of Ki67 positive cells in the designated regions of the CVP epithelium of control and AS-ODN-treated specimens is presented in the form of bar graph and table (Fig. 4e, Ki67). In addition, the number of Ki67 positive cells in the condensed mesenchyme of AS-ODN-treated CVP domes was decreased (Fig. 4c) compared to controls (Fig. 4a), indicating a reduction in cell proliferation in the mesenchyme. However, there was an increase in the number of Ki67 positive cells in the mesenchyme immediately adjacent to the trench epithelium in AS-ODN-treated tissues (Fig. 4c) compared to controls (Fig. 4a). Cell death was reduced

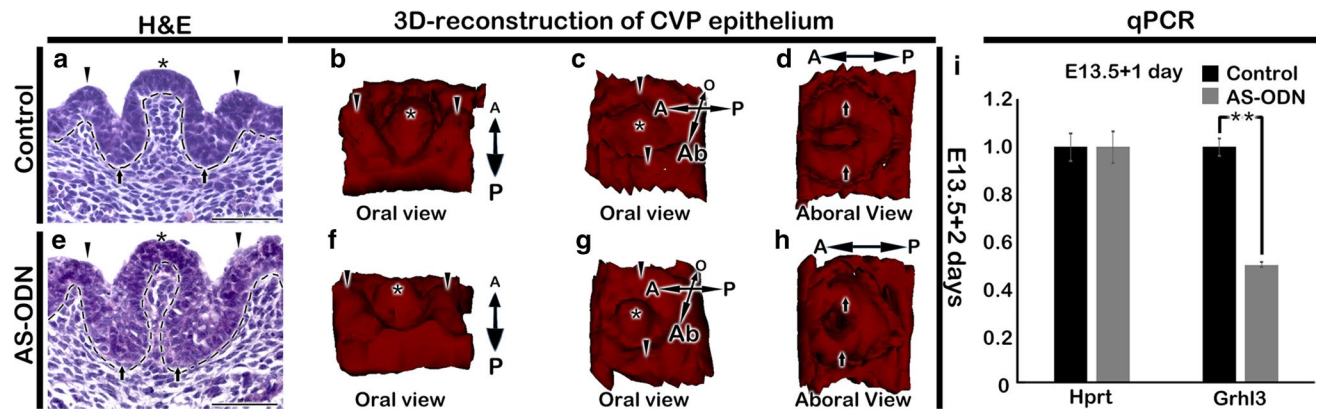


Fig. 2 Altered morphology of the CVP following *Grhl3* knockdown in vitro. H&E staining shows the epithelial structure of a control and AS-ODN-treated CVP (**a**, **e**). Compared to the control (**a**), the AS-ODN-treated CVP shows a more rounded dome and more deeply invaginated trench epithelium (**e**). A frontal section and 3D reconstruction of the CVP shows the altered shape and dome size in AS-

ODN-treated (**e–h**) compared to controls (**a–d**). *Grhl3* expression is down regulated by about 50 % after treatment with AS-ODN as detected by RT-qPCR (**i**). A, anterior; Ab, aboral; O, oral; P, posterior. Dotted lines indicate basement membrane. Arrows, arrowheads and asterisk represent trench, vallum and apex epithelium, respectively. ** $P < 0.05$. Scale bars 50 μm (**a**, **e**)

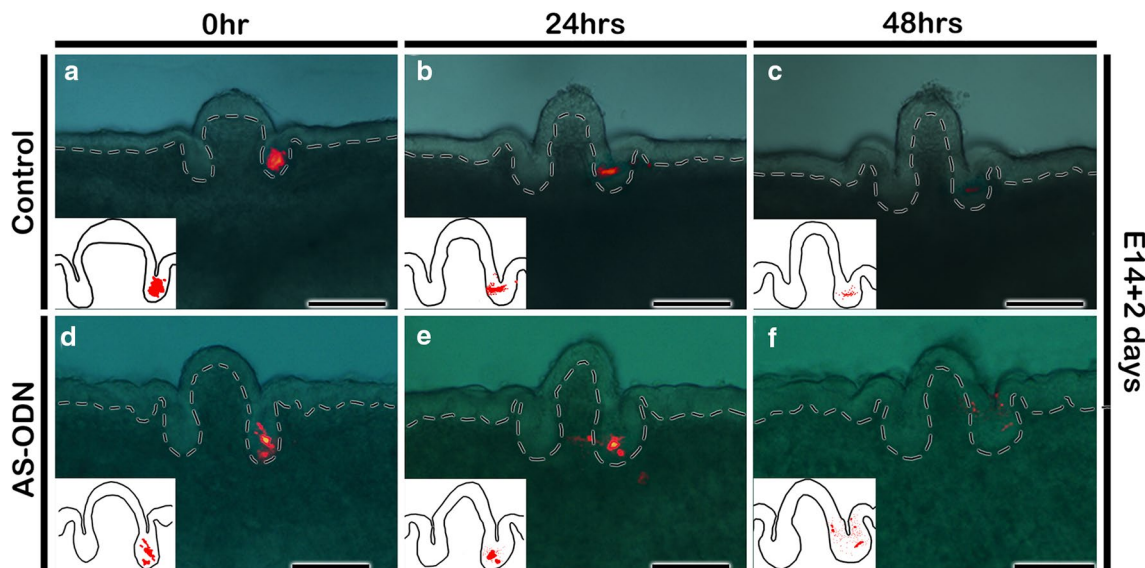


Fig. 3 Cell movement tracking following DiI microinjection in an in vitro slice culture. DiI labeling of cells in the exposed trench of an E14 CVP slice culture (**a**, **d**): Altered proliferation and migration pattern of DiI-labeled cells in control (**b**, **e**) and AS-ODN-treated CVPs (**e**, **f**) after culture for 24 and 48 h. Reduced DiI intensity and scattered DiI-labeled cells in the AS-ODN-treated (**f**) compared to con-

trol (**c**) tissues are indicative of extensive cell proliferation and migration after 48 h in culture. Insets are a schematic depiction of the DiI labeling showing proliferation and migration patterns at respective time periods. Dotted lines indicate basement membrane. Scale bars 100 μm (**a–f**)

in the apex, trench wall, and vallum epithelium of the CVP following AS-ODN-treatment (Fig. 4d) compared to controls (Fig. 4b) as indicated by a reduction in the number of apoptotic cells in the treated tissues. The number of TUNEL positive cells in the designated regions of the CVP epithelium of control and AS-ODN-treated specimens is presented in the form of bar graph and table (Fig. 4e, TUNEL).

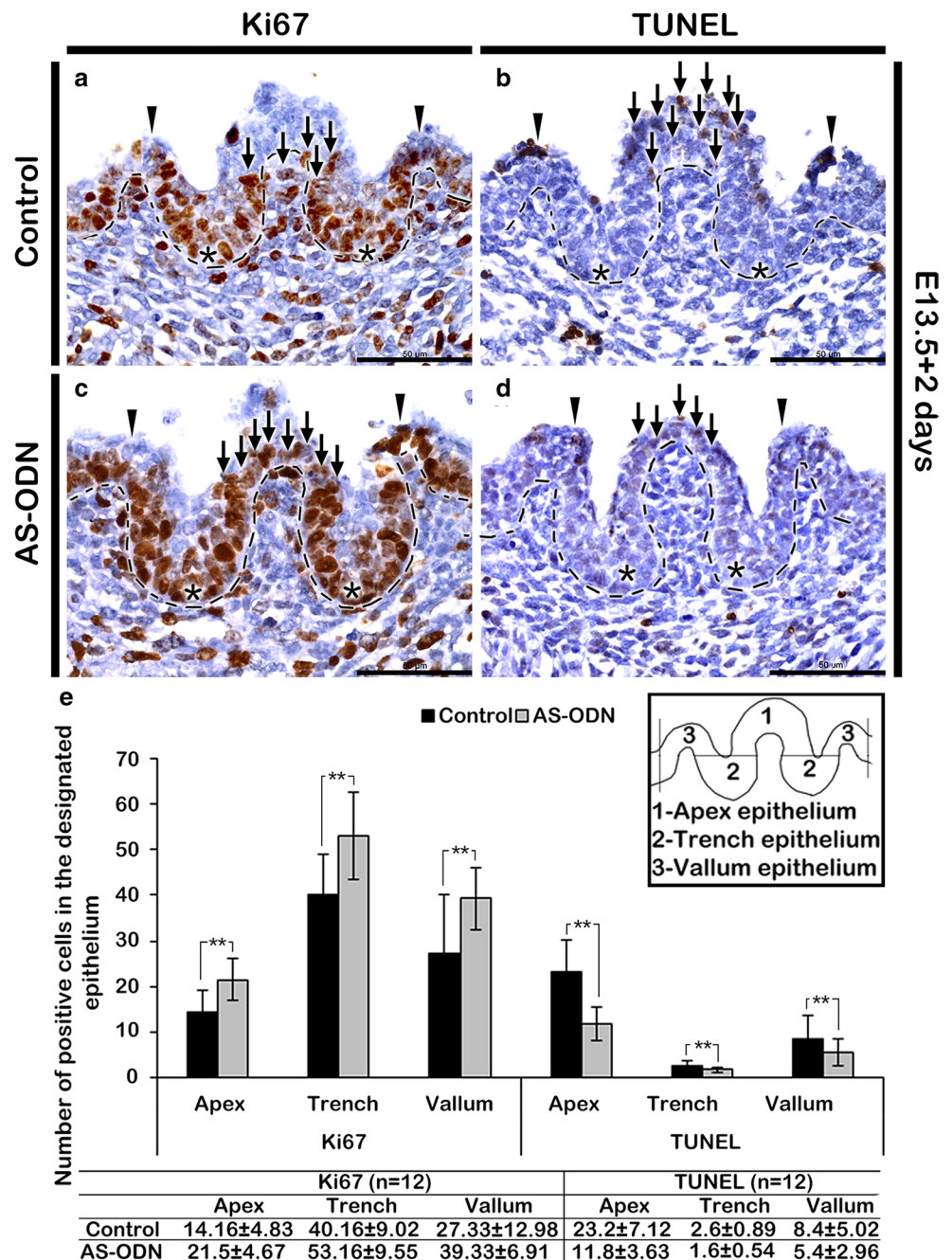
Altered localization patterns of epithelial cell adhesion and rearrangement-related factors following *Grhl3* knockdown

To examine the role of *Grhl3* in epithelial cell adhesion and cell rearrangement, we performed immunohistochemistry for ROCK1 (Fig. 5a, d) and E-cadherin (Fig. 5c, f) in AS-ODN-treated and control CVP tissues. In addition, we

used phalloidin staining to detect actin filaments (Fig. 5b, e). The intensity of ROCK1 localization was reduced in the epithelium of AS-ODN-treated CVP specimens (Fig. 5d) compared to controls (Fig. 5a). Interestingly, ROCK1 was almost absent in the apex and vallum epithelium of AS-ODN treated specimens (Fig. 5d) compared to controls (Fig. 5a), while the intensity was reduced in the trench epithelium of AS-ODN-treated specimens (Fig. 5d) compared to controls (Fig. 5a). Consistent with this, there was a decrease in the intensity of actin filament staining in the apex and vallum of AS-ODN-treated CVP (Fig. 5e) compared to that of controls

(Fig. 5b). Conversely, the intensity of actin filament staining was increased in the basement membrane of the invaginated epithelium in AS-ODN-treated CVP (Fig. 5e) compared to controls (Fig. 5b). Furthermore, the epithelial cell adhesion molecule E-cadherin was also altered following AS-ODN treatment. Consistent with ROCK1, E-cadherin was absent in the apex and vallum epithelium of AS-ODN-treated CVP (Fig. 5f); however, that was not the case in the controls (Fig. 5c). In contrast, an increase in E-cadherin intensity was observed in the trench epithelium of AS-ODN-treated tissues (Fig. 5f) compared to controls (Fig. 5c).

Fig. 4 Altered cell proliferation and apoptosis after *Grhl3* knockdown. Ki67 immunostaining of an AS-ODN-treated CVP (c) shows an increase in the number of Ki67 positive cells in the apex, trench, and vallum epithelium compared to the control (a). The number of apoptotic cells in the apex, trench and vallum epithelium decreased after *Grhl3* knockdown (d) compared to controls (b) as detected by a TUNEL assay. Graph shows the number of Ki67 and TUNEL positive cells in the apex, trench, and vallum epithelium (e). Inset in (e) is a schematic diagram showing the regions of the CVP epithelium used to count the positive cells. Dotted lines indicate basement membrane. Arrows indicate positive cells in the apex epithelium. Arrowheads and asterisk represent vallum and trench epithelium, respectively. Scale bars 50 μm (a–d). ***P* < 0.05



Altered expression of Shh-, Wnt-, and apoptosis-related signaling molecules following Grhl3 knockdown

In order to define the molecular mechanisms that are regulated by *Grhl3*, E13.5 CVPs were treated with AS-ODN to knockdown *Grhl3*. After 1 day of in vitro roller culture, the expressions of *Shh*-, *Wnt*-, and apoptosis-related signaling molecules were examined using RT-qPCR. *Shh* and *Wnt11* have been shown to be involved in CVP development (Mistretta et al. 2003; Jaskoll et al. 2004; Lee et al. 2006; Kim et al. 2009; Wells et al. 2011). Expression of *Shh* and the related factors *Ptch1* and *Gli3* was up-regulated following *Grhl3* knockdown, as was expression of the Wnt-signaling molecules *Wnt11* and *Ctnnb1*. Similarly, the

apoptosis-related factors *Bak1*, *Bcl2*, and *Casp3* showed increased expression levels, whereas *Casp8*, an extrinsic apoptosis factor, was downregulated following *Grhl3* knockdown (Fig. 6).

Discussion

CVP morphogenesis occurs via sequential and reciprocal interactions between the epithelium and underlying mesenchyme, which are mediated by a number of conserved signaling molecules including Wnt, Shh, Fgf, Tgf, and Tnf, along with their downstream transcription factors (Pispa and Thesleff 2003; Mikkola 2007). The first morphological

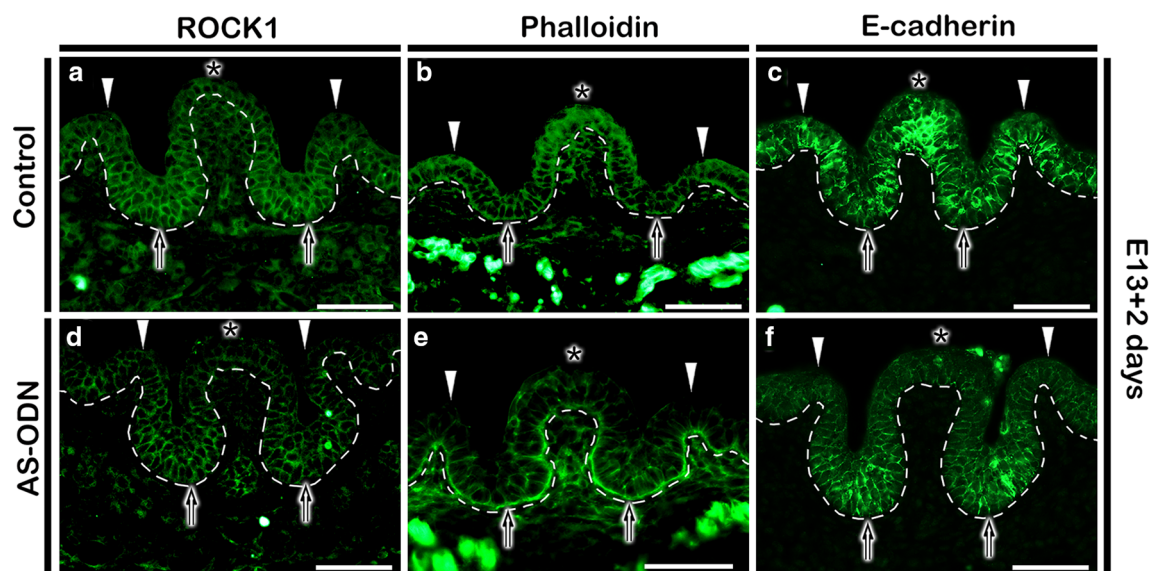


Fig. 5 Localization patterns of ROCK1, phalloidin, and E-cadherin in the CVP following *Grhl3* knockdown. ROCK1 is weakly localized in the AS-ODN-treated tissue (d) compared to the control (a). Increased intensity of phalloidin staining in the basement membrane of AS-ODN-treated specimens (e) compared to controls (b). E-cad-

herin is altered in AS-ODN-treated specimens (f) compared to controls (c). Dotted lines indicate basement membrane. Arrows, arrowheads and asterisk represent trench, vallum, and apex epithelium, respectively. Scale bars 50 μ m (a–f)

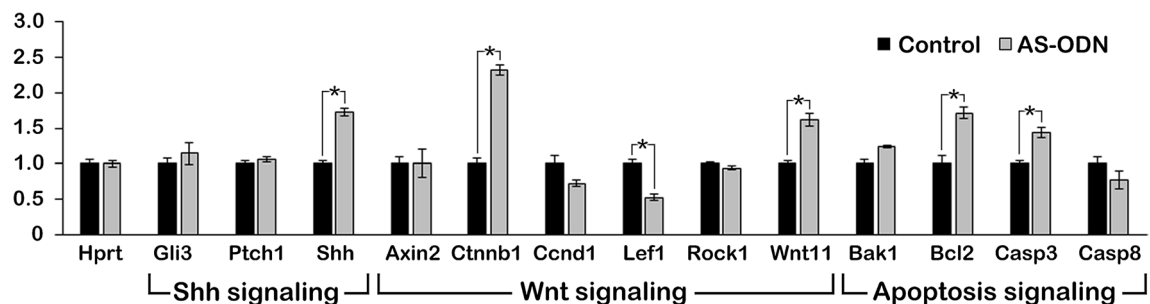


Fig. 6 Altered expression of signaling molecules following *Grhl3* knockdown in vitro as detected by RT-qPCR. Up-regulation of *Shh* and related factors along with *Wnt11*, *Ctnnb1* and anti-apoptotic fac-

tor *Bcl2* after *Grhl3* knockdown. Extrinsic apoptosis factor *Casp8* is downregulated after *Grhl3* knockdown. * $P < 0.05$

sign of CVP formation is observed at E13 (AhPin et al. 1989) and acquires a “dome-shaped” appearance, with subsequent invagination of the adjacent epithelium by E15 (Jitpukdeebodindra et al. 2002). In the current study, we examined the expression pattern of *Grhl3* in the CVP at E13.5, E14.5, and E15.5. Our observations are consistent with the expression pattern for the oral epithelium reported previously (Auden et al. 2006). Based on the expression pattern, we hypothesized that *Grhl3* could have a specific role in formation of CVP epithelial structure during embryogenesis such as structural formation with epithelial invaginations.

To evaluate this hypothesis, we employed the stage- and tissue-specific knockdown of *Grhl3* by using AS-ODN or siRNA treatments during in vitro organ cultivation to understand the detailed roles of *Grhl3* in the circumvallate papilla morphogenesis. The previous reports on role of *Grhl3* from knockout mouse model showed the requirement of this gene in epithelial integrity and periderm formation, in which, however, dynamicity of morphogenesis of various organs has not been revealed and tongue circumvallate papilla is one of them (Ting et al. 2005a, b; De la Garza et al. 2013). Knocking down of gene using AS-ODN during in vitro organ cultivation at specific stage gives insight into the developmental role of that gene in the stage-specific morphogenesis of organs and advantageous over knock out model which interferes entire signaling regulations starting from the organogenesis. So, the in vitro organ cultivation of stage-specific tissues with functional analysis would provide plausible answers to understand the signaling integrations in tissue regeneration.

To track the morphological development of the CVP, and to determine the role of *Grhl3* in this process, we cultured tongues from E13.5 embryos, in the presence or absence of AS-ODNs against *Grhl3*, for 2 days. Approximately 50 % of *Grhl3* was knocked down by AS-ODNs against *Grhl3* after in vitro organ culture for 1 day, as confirmed by RT-qPCR; knocking down a gene to this extent alters the signaling regulation in a developing organ, thus allowing visualization of any morphological alterations. Further, we tested siRNA against *Grhl3*; however, this resulted in only about 25 % *Grhl3* knockdown, as confirmed by RT-qPCR, and caused similar alterations in CVP morphogenesis (data not shown). Hence, AS-ODN treatment was employed throughout the study to knockdown *Grhl3*. After 2 days of in vitro culture, the morphology of the E13.5 control CVP resembled that of an E15 in vivo CVP (data not shown). However, slight retardation was observed in the development which could be due to time constraints and lack of the complete oral environmental conditions that could not be fulfilled during in vitro cultivation. As expected, the AS-ODN-treated CVP showed remarkable alteration in structure compared to the control, and this was further evaluated

using computer-aided three-dimensional (3D) reconstructions. Although diverse cutting-edge techniques, including micro-computed tomography and confocal microscopy, are available to examine detailed morphology, these processes require expensive instruments, which ultimately increases the performance cost. Therefore, we attempted to evaluate the CVP architecture using a 3D computer-aided reconstruction method, which has been used in a number of anatomical and histological studies (Kim et al. 2011). We obtained 3D images using reconstruction software to align serial frontal histological sections of cultured control and AS-ODN-treated CVPs. This provided us with clear images of the altered morphology in the AS-ODN-treated specimens compared to the controls. Data from the control CVPs in this experiment were consistent with that from a previous report by Sohn et al. (2011).

After observing these distinct alterations in morphology, we investigated the cell dynamics that could have caused these changes. To determine changes in cell migration, we labeled cells with DiI and tracked them during CVP development in vitro. In addition, cell proliferation and apoptosis were examined in E13.5 CVPs after 48 h of in vitro culture. Cell proliferation is extensive from the early stage of tongue development and is active throughout embryogenesis, while apoptosis, which is restricted to the upper layer of epithelium, occurs later in embryogenesis (Nagata and Yamane 2004; Nie 2005). Previous reports have suggested that cell proliferation and migration are major events in CVP morphogenesis (Jitpukdeebodindra et al. 2002) and shown that *Grhl3* plays a role in proliferation, migration, and apoptosis (Ting et al. 2005a, b; Hislop et al. 2008; Darido and Jane 2010; Caddy et al. 2010; Lukosz et al. 2011; Georgy et al. 2015; Zhao et al. 2016). Therefore, we examined these cellular events in the developing CVP, following knockdown of *Grhl3*. As expected, DiI-labeling experiments showed scattered DiI-labeled cells, with decreased intensity in the AS-ODN-treated specimens compared to the controls, suggesting that epithelial cells in the trench wall undergo hyperproliferation and altered migration because of *Grhl3* knockdown. Consistent with this, Ki67 immunostaining revealed increased proliferation in the epithelium of AS-ODN-treated specimens. In addition, mesenchymal cell proliferation was affected by knockdown of *Grhl3*, implying the existence of an epithelial-mesenchymal interactions in the AS-ODN-treated specimens. In contrast to cell proliferation, the AS-ODN-treated CVP specimens showed a reduction in cell apoptosis compared to controls. Thus, the extensive proliferation, decreased apoptosis, and altered cell migration could explain the thickened and more deeply invaginated trench epithelium that was observed in the AS-ODN-treated tissues. These results further suggest that *Grhl3* may also facilitate the branching morphogenesis of von Ebners' minor salivary

gland, which occurs after the epithelial invagination (Kim et al. 2009). Our results from the *Grhl3* knockdown experiments are consistent with reports of hyperproliferating epidermal cells in *Grhl3* null mice (Ting et al. 2005a, b), and more recently, with a report showing that *Grhl3* deletion results in hyperproliferation, along with increased thickness of the tongue epithelium (Georgy et al. 2015). Furthermore, reduced expression of *Grhl3* has been linked to an increased risk of skin cancer due to altered epithelial-mesenchymal interactions (Darido et al. 2011), which would be consistent with the cell proliferation data from the present study.

The structural integrity of an organ is maintained by the cytoskeleton. A number of developmental events that occur during embryogenesis, including yolk sac formation, eyelid closure, neural tube closure, and renal tubulogenesis, involve cell movement that occurs by the mechanism of convergent extension (Ybot-Gonzalez et al. 2007). This process is controlled by the planar cell polarity (PCP) pathway, to which *Grhl3* is reportedly an important contributor (Caddy et al. 2010). *Grhl3* is thought to activate *RhoGEF19*, which functions as a direct activator of *RhoA* and thus leads to actin polymerization and cytoskeletal arrangement (Darido and Jane 2010; Dworkin et al. 2011). These reports led us to investigate the possible role of *Grhl3* in modulating cytoskeletal structure formation in the epithelium during organogenesis. The relationship between *Grhl3* signaling and ROCK1, E-cadherin, and actin filament formation during CVP morphogenesis was examined using AS-ODNs to knockdown *Grhl3*. At E13.5 CVPs, organ cultures were grown with or without AS-ODN treatment for 2 days in vitro. The localization pattern of ROCK1, E-cadherin, and actin filament formation was altered following *Grhl3* knockdown, suggesting that *Grhl3* may modulate CVP structure formation via the regulation of ROCK1, E-cadherin, and actin filament formation. These data are consistent with a recent report showing that *Grhl3* is an important factor in epithelial organogenesis, and specifically for activating E-cadherin and mediating mesenchymal–epithelial transition (Alotaibi et al. 2015).

Shh and *Wnt11* signaling have been reported to be involved in structural formation of the CVP (Kim et al. 2009). To determine the potential relationship between *Grhl3* and *Shh* and *Wnt11*, we knocked down *Grhl3* in an in vitro culture system and performed RT-qPCR analysis. Our observations revealed that *Grhl3* knockdown affected the activity of *Shh* and *Wnt11* signaling, which could in turn lead to the cellular rearrangements that we observed in the epithelium. It is interesting to note that the activity of both *Shh* and *Wnt11* have been shown to increase after the loss of *Grhl3* function, though these molecules are antagonists of each other (Cho et al. 2011). However, this could be explained by the presence of a Wnt–Shh

negative feedback mechanism that regulates their function (Ahn et al. 2010). In addition, RT-qPCR analysis revealed altered expression of apoptosis-related signaling molecules following *Grhl3* knockdown. Caspase-3, an apoptosis executioner Caspase, showed increased expression following *Grhl3* knocking down. As were examined in previous reports, the increased expression of Caspase-3 does not necessarily enhance apoptosis and is related to various other non-apoptotic biological processes (Ishizaki et al. 1998; Fernando et al. 2002; Donato et al. 2014). Moreover, the function of *Caspase-3* depends on the level of initiator Caspase, Caspase-8, which showed the down regulated expression (Favaloro et al. 2012), resulting in the decreased apoptosis as observed with TUNEL staining. Furthermore, the decreased apoptotic activity could be explained due to increased expression of the anti-apoptotic factor *Bcl2* following *Grhl3* knocking down. As reported previously, *Grhl3* promotes periderm formation over the differentiating epithelium during embryogenesis (De La Garza et al. 2013), and a defect in *Grhl3* leads to improper epithelial barrier formation (Ting et al. 2005a, b). A defective barrier would result in bilateral adhesion of the oral epithelium, perturbing normal palate development (Peyrard-Janvid et al. 2014). Our data showing *Grhl3* expression in the developing CVP epithelium and altered apoptosis signaling in the superficial layer of the CVP epithelium in AS-ODN-treated specimens further suggest that *Grhl3* has a crucial role in oral periderm development. However, these results would not be related to secondary consequences of the disruption of epithelial integrity.

In summary, our observations suggest that *Grhl3* has a significant role in CVP epithelial structure morphogenesis, and that it functions by controlling cell proliferation, migration, and apoptosis via regulation of ROCK1, E-cadherin, and actin filament formation. These results would be explained by reported earlier that ROCK1 is known to integrate with E-cadherin via p120-catenin which stabilizes β -catenin and actin filament formation resulting in the inhibition of cell proliferation (Smith et al. 2011). Furthermore, Rock1 regulates actin cytoskeleton, cell migration, cell survival, and proliferation through G proteins signaling (Horani et al. 2013). Besides this, rearrangement of actin filament is induced by E-cadherin to support contractility during apoptosis of epithelial cells (Michael et al. 2016). In addition, *Grhl3* may play a vital role in morphogenesis of the glandular epithelium. Further, we conclude that *Grhl3* has a regulatory effect on the Shh and Wnt pathways that are involved in patterning, tissue polarity, and cell fate specification in many developmental processes (Huelsen and Birchmeier 2001). The cellular events that comprise CVP morphogenesis, including cell proliferation, migration, and apoptosis, and are modulated by *Grhl3*, could

represent a good model for studying cell patterning and differentiation in a range of organs during embryogenesis. Furthermore, regulation of cell adhesion molecules and actin filaments by *Grhl3*, along with proliferation and apoptosis, could play a crucial role in tumor biology and epithelial tissue engineering.

Acknowledgments This study was supported by a National Research Foundation of Korea (NRF) grant funded by the Korean Government (MSIP; No. 2008-0062282) and the National Research Foundation of Korea (Grant NRF-2012R1A1A2044113) funded by the Ministry of Education, Science and Technology, Republic of Korea.

Compliance with ethical standards

Conflict of interest The authors declare that they have no conflicts of interest.

References

- Ahn Y, Sanderson BW, Klein OD, Krumlauf R (2010) Inhibition of Wnt signaling by wise (Sostdc1) and negative feedback from Shh controls tooth number and patterning. *Development* 137:3221–3231
- AhPin P, Ellis S, Arnott C, Kaufman MH (1989) Prenatal development and innervation of the circumvallate papilla in the mouse. *J Anatomy* 162:33–42
- Alotaibi H, Basilicata MF, Shehwana H, Kosowan T, Schreck I, Braeutigam C, Konu O, Brabletz T, Stemmler MP (2015) Enhancer cooperativity as a novel mechanism underlying the transcriptional regulation of E-Cadherin during mesenchymal to epithelial transition. *Biochim Biophys Acta* 1849:731–742
- Auden A, Caddy J, Wilanoswski T, Ting SB, Cunningham JM, Jane SM (2006) Spatial and temporal expression of the Grainyhead-like transcription factor family during murine development. *Gene Expr Patterns* 6(8):964–970
- Biggs LC, Mikkola ML (2014) Early inductive events in ectodermal appendage morphogenesis. *Semin Cell Dev Biol* 25–26:11–21
- Boglev Y, Wilanoswski T, Caddy J, Parekh V, Auden A, Darido C, Hislop NR, Canqkrama M, Ting SB, Jane SM (2011) The unique and cooperative roles of the Grainy head-like transcription factors in epidermal development reflect unexpected target gene specificity. *Dev Biol* 349:512–522
- Caddy J, Wilanoswski T, Darido C, Deorkin S, Ting SB, Zhao Q, Rank G, Auden A, Srivastava S, Papenfuss TA, Murdoch JN, Humbert PO, Parekh V, Boulos N, Weber T, Zuo J, Cunningham JM, Jane SM (2010) Epidermal wound repair is regulated by the planar cell polarity signaling pathway. *Dev Cell* 19(1):138–147
- Cho SW, Kwak S, Woolley TE, Lee MJ, Kim EJ, Baker RE, Kim HJ, Shin JS, Tickle C, Maini PK, Jung HS (2011) Interactions between Shh, Sostdc1 and Wnt signaling and a new feedback loop for spatial patterning of the teeth. *Development* 138:1807–1816
- Darido C, Jane SM (2010) Grhl3 and GEF10 in the front rho. *Small GTPases* 1(2):104–107
- Darido C, Georgy SR, Wilanoswski T, Dworkin S, Auden A, Zhao Q, Rank G, Srivastava S, Finlay MJ, Papenfuss AT, Pandolfi PP, Pearson RB, Jane SM (2011) Targeting of the tumor suppressor GRHL3 by a miR-21-dependent proto-oncogenic network results in PTEN loss and tumorigenesis. *Cancer Cell* 20(5):635–648
- De la Garza G, Schleiffarth JR, Dunnwald M, Mankad A, Weirather JL, Bonde G, Butcher S, Mansour TA, Kousa YA, Fukazawa CF, Houston DW, Manak JR, Schutte BC, Wagner DS, Cornell RA (2013) Interferon regulatory factor 6 promotes differentiation of the periderm by activating expression of Grainyhead-like 3. *J Invest Dermatol* 133:68–77
- Donato AL, Huang Q, Liu X, Li F, Zimmerman MA, Li CY (2014) Caspase 3 promotes surviving melanoma tumor cell growth after cytotoxic therapy. *J Invest Dermatol* 134:1686–1692
- Dworkin S, Jane SM, Darido C (2011) The planar cell polarity pathway in vertebrate epidermal development, homeostasis and repair. *Organogenesis* 7(3):202–208
- Favaloro B, Allocati N, Graziano V, Di Ilio C, De Laurenzi V (2012) Role of apoptosis in disease. *Aging (Albany NY)* 4(5):330–349
- Fernando P, Kelly JF, Balazsi K, Slack RS, Megey LA (2002) Caspase 3 activity is required for skeletal muscle differentiation. *Proc Natl Acad Sci USA* 99:11025–11030
- Gao Y, Toska E, Denmon D, Roberts SGE, Medler KF (2014) WT1 regulates the development of the posterior taste field. *Development* 141:2271–2278
- Georgy SR, Cangkrama M, Srivastava S, Partridge D, Auden A, Dworkin S, McLean CA, Jane SM, Darido C (2015) Identification of a novel proto-oncogenic network in head and neck squamous cell carcinoma. *J Natl Cancer Inst.* doi:10.1093/jnci/djv152
- Gustavsson P, Copp AJ, Greene ND (2008) Grainyhead genes and mammalian neural tube closure. *Birth Defects Res A Clin Mol Teratol* 82:728–735
- Hislop NR, Caddy J, Ting SB, Auden A, Vasudevan S, King SL, Lindeman GJ, Visvader JE, Cunningham JM, Jane SM (2008) Grhl3 and Lmo4 play coordinate roles in epidermal migration. *Dev Biol* 321:263–272
- Horani A, Nath A, Wasserman MG, Huang T, Brody SL (2013) Rho-associated protein kinase inhibition enhances airway epithelial basal-cell proliferation and lentivirus transduction. *Am J Respir Cell Mol Biol* 49(3):341–347
- Huelsken J, Birchmeier W (2001) New aspects of Wnt signaling pathways in higher vertebrates. *Curr Opin Genet Dev* 11:547–553
- Ishizaki Y, Jacobson MD, Raff MC (1998) A role for caspases in lens fiber differentiation. *J Cell Biol* 140:153–158
- Jaskoll T, Leo T, Witcher D, Ormestad M, Astorga J, Bringas P Jr, Carlsson P, Melnick M (2004) Sonic hedgehog signaling plays an essential role during embryonic salivary gland and epithelial branching morphogenesis. *Dev Dyn* 229:722–732
- Jitpukdeebodindra S, Chai Y, Snead ML (2002) Developmental patterning of the circumvallate papilla. *Int J Dev Biol* 46:755–763
- Kim JY, Lee MJ, Cho KW, Lee JM, Kim YJ, Kim JY, Jung HI, Cho JY, Cho SW, Jung HS (2009) Shh and Rock1 modulate the dynamic epithelial morphogenesis in circumvallate papilla development. *Dev Biol* 325:273–280
- Kim JN, Koh KS, Lee E, Park SC, Song WC (2011) The morphology of the rat vibrissal follicle-sinus complex revealed by three-dimensional computer-aided reconstruction. *Cells Tissues Organs* 193:207–214
- Kist R, Watson M, Crosier M, Robinson M, Fuchs J, Reichelt J, Peters H (2014) The formation of endoderm-derived taste sensory organs requires a Pax9-dependent expansion of embryonic taste bud progenitor cells. *PLoS Genet* 10(10):e1004709. doi:10.1371/journal.pgen.1004709
- Lee MJ, Kim JY, Lee SI, Sasaki H, Lunny DP, Lane EB, Jung HS (2006) Association of Shh and Ptc with keratin localization in the initiation of the formation of circumvallate papilla and von Ebner's gland. *Cell Tissue Res* 325:253–261
- Liu H, Leslie EJ, Jia Z, Smith T, Eshete M, Butali A, Dunnwald M, Murray J, Cornell RA (2016) Irf6 directly regulates Klf17 in zebrafish periderm and Klf4 in murine oral epithelium, and

- dominant-negative KLF4 variants are present in patients with cleft lip and palate. *Hum Mol Genet* 25(4):766–776
- Lukosz M, Mlynek A, Czypiorski P, Altschmied J, Haendeler J (2011) The transcription factor Grainyhead like 3 (GRHL3) affects endothelial cell apoptosis and migration in a NO-dependent manner. *Biochem Biophys Res Commun* 412:648–653
- Michael M, Meiring JC, Acharya BR, Matthews DR, Verma S, Han SP, Hill MM, Parton RG, Gomez GA, Yap AS (2016) Coronin 1B reorganizes the architecture of F-actin networks for contractility at steady-state and apoptotic adherens junctions. *Dev Cell* 37(1):58–71
- Mikkola ML (2007) Genetic basis of skin appendage development. *Semin Cell Dev Biol* 18(2):225–236
- Mistretta CM, Liu HX, Gaffield W, MacCallum DK (2003) Cyclopamine and jervine in embryonic rat tongue cultures demonstrate a role for Shh signalling in taste papilla development and patterning: fungiform papillae double in number and form in novel locations in dorsal lingual epithelium. *Dev Biol* 254:1–18
- Nagata J, Yamane A (2004) Progress of cell proliferation in striated muscle tissues during development of the mouse tongue. *J Dent Res* 83(12):926–929
- Neupane S, Sohn WJ, Rijal G, Lee YJ, Lee S, Yamamoto H, An CH, Cho SW, Lee Y, Shin HI, Kwon TY, Kim JY (2014) Developmental regulations of *Perp* in mice molar morphogenesis. *Cell Tissue Res* 358(1):109–121
- Neupane S, Sohn WJ, Gwon GJ, Kim KR, Lee S, An CH, Suh JY, Shin HI, Yamamoto H, Cho SW, Lee Y, Kim JY (2015) The role of *APCDD1* in epithelial rearrangement in tooth morphogenesis. *Histochem Cell Biol* 144(4):377–387
- Nie X (2005) Apoptosis, proliferation and gene expression patterns in mouse developing tongue. *Anat Embryol (Berl)* 210(2):125–132
- Otsu K, Kishigami R, Fujiwara N, Ishizeki K, Harada H (2011) Functional role of Rho-kinase in ameloblast differentiation. *J Cell Physiol* 226(10):2527–2534
- Petersen CI, Jheon AH, Mostowfi P, Charles C, Ching S, Thirumangalathu S, Barlow LA, Klein OD (2011) FGF signaling regulates the number of posterior taste papillae by controlling progenitor field size. *PLoS Genet* 7(6):e1002098. doi:10.1371/journal.pgen.1002098
- Peyrard-Janvid M, Leslie EJ, Kousa YA, Smith TL, Dunnwald M, Magnusson M, Lentz BA, Unneberg P, Fransson I, Koillinen HK, Rautio J, Pegelow M, Karsten A, Basel-Vanagaite L, Gordon W, Andersen B, Svensson T, Murray JC, Cornell RA, Kere J, Schutte BC (2014) Dominant mutations in *GRHL3* cause Van der Woude Syndrome and disrupt oral periderm development. *Am J Hum Genet* 94:23–32
- Pispa J, Thesleff I (2003) Mechanisms of ectodermal organogenesis. *Dev Biol* 262:195–205
- Smith AL, Dohn MR, Brown MV, Reynolds AB (2011) Association of Rho-associated protein kinase 1 with E-cadherin complexes is mediated by p120-catenin. *Mol Biol Cell* 23(1):99–110
- Sohn WJ, Gwon GJ, An CH, Moon C, Bae YC, Yamamoto H, Lee S, Kim JY (2011) Morphological evidences in circumvallate papilla and von Ebner's gland development in mice. *Anat Cell Biol* 44(4):274–283
- Sohn WJ, Ji YR, Kim HS, Gwon GJ, Chae YM, An CH, Park HD, Jung HS, Ryoo ZY, Lee S, Kim JY (2012) *Rgs 19* regulates mouse palatal fusion by modulating cell proliferation and apoptosis in the MEE. *Mech Dev* 129:244–254
- Sohn WJ, Gwon GJ, Kim HS, Neupane S, Cho SJ, Lee JH, Yamamoto H, Choi JY, An CH, Lee Y, Shin HI, Lee S, Kim JY (2015) Mesenchymal signaling in dorsoventral differentiation of palatal epithelium. *Cell Tissue Res* 362:541–556
- Suzuki Y, Ikeda K, Kawakami K (2011) Development of gustatory papillae in the absence of *Six1* and *Six4*. *J Anat* 219:710–721
- Ting SB, Caddy J, Hislop N, Wilanoswski T, Auden A, Zhao LL, Ellis S, Kaur P, Uchida Y, Holleran WM, Elias PM, Cunningham JM, Jane SM (2005a) A homolog of drosophila grainyhead is essential for epidermal integrity in mice. *Science* 308:411–413
- Ting SB, Caddy J, Wilanowski T, Auden A, Cunningham JM, Elias PM, Holleran WM, Jane SM (2005b) The epidermis of *grhl3*-null mice displays altered lipid processing and cellular hyperproliferation. *Organogenesis* 2:33–35
- Wells KL, Mou C, Headon DJ, Tucker AS (2011) Defects and rescue of the minor salivary glands in *Eda* pathway mutants. *Dev Biol* 349:137–146
- Ybot-Gonzalez P, Savery D, Gerrelli D, Signore M, Mitchell CE, Faux CH, Greene ND, Copp AJ (2007) Convergent extension, planar-cell-polarity signalling and initiation of mouse neural tube closure. *Development* 134(4):789–799
- Zhao P, Guo S, Tu Z, Di L, Zha X, Zhou H, Zhang X (2016) *Grhl3* induces human epithelial tumor cell migration and invasion via downregulation of E-cadherin. *Acta Biochim Biophys Sin (Shanghai)* 48(3):266–274